LAWRENCE
LIVERMORE
NATIONAL
LABORATORY

UCRL-JRNL-201991

Correlated Nitrogen And Carbon Anomalies In An Anhydrous Interplanetary Dust Particles

C. Floss, F. J. Stadermann, J. Bradley, Z. Dai, G. Graham

January 26, 2004

Science

Correlated Nitrogen and Carbon Anomalies in an Anhydrous Interplanetary Dust Particle

Christine Floss[1], Frank J. Stadermann[1] John Bradley[2], Zurong Dai[2], Sasa Bajt[2], Giles Graham[2]

[1]Laboratory for Space Sciences, Washington University

St. Louis, MO 63130

[2]Institute for Geophysics and Planetary Physics,

Lawrence Livermore National Laboratory

Livermore, CA 94550

The presence of a ^{13}C depletion associated with a ^{15}N enrichment in an anhydrous interplanetary dust particle provides the first observation of correlated C and N isotopic anomalies in organic matter from an IDP and requires as yet unidentified interstellar fractionation processes that can produce both effects simultaneously.

Submitted to Science

Fall 2003

Abstract

Given the ubiquitous presence of H and N isotopic anomalies in interplanetary dust particles (IDPs) and their probable association with carbonaceous material, the lack of similar isotopic anomalies in C has been a major conundrum. We report here the first observation of correlated N and C isotopic anomalies in organic matter from an anhydrous non-cluster IDP. The ^{15}N composition of the anomalous region is the highest seen to date in an IDP and is accompanied by a moderate depletion in ^{13}C. Theoretical models suggest that low temperature formation of organic compounds in cold interstellar molecular clouds does produce C and N fractionations, but it remains to be seen if these models can reproduce the specific effects we observe here.

Introduction

Interstellar molecular clouds are the principal formation sites of organic matter in the Galaxy. A variety of simple molecules, such as CH_4, CH_3OH, and H_2CO, are produced in dense cold (10 – 30 K) clouds (*1*). At such low temperatures, where the difference in chemical binding energy exceeds thermal energy, mass fractionation results in molecules with isotopic ratios that can be anomalous relative to solar system values (*1, 2*). Such anomalous ratios potentially provide a 'fingerprint' for abiotic interstellar organic matter that was incorporated into the solar system and survives in cosmically primitive materials such as interplanetary dust particles (IDPs).

IDPs are fragments of comets and asteroids collected in the Earth's stratosphere. These particles are complex assemblages of primitive solar system material and are the repositories of various isotopic anomalies (*2-4*). Deuterium enhancements in IDPs are interpreted as the result of extreme chemical fractionation in cold molecular clouds (*5*) and D/H ratios in some IDPs approach the values observed in interstellar molecules (*6*), suggesting the intact survival of some molecular cloud material. Nitrogen isotopic anomalies, in the form of ^{15}N enrichments, are also common in IDPs (and in some primitive meteorites) and are generally postulated to result from low temperature interstellar chemistry (*2, 7*). This origin is complicated by the fact that N isotopic fractionation has not been observed in the interstellar medium and that anomalous N can also have a nucleosynthetic origin. However, recent work has shown that chemical

reactions in dense molecular gases can produce elevated $^{15}N/^{14}N$ ratios (*8, 9*), although the maximum enhancements still fall short of observed ^{15}N enrichments in IDPs (*10, 11*).

The specific phases hosting isotopic anomalies in IDPs remain poorly characterized. Although other carriers have also been implicated (*12*), organic compounds appear to be the source of many of the D and ^{15}N enrichments (*13-15*). It is puzzling, therefore, that prior to this study the H and N isotopic anomalies in IDPs have not been accompanied by corresponding C anomalies, despite numerous C isotopic measurements (*4*).

C and N Isotopic Imaging

As part of an ongoing survey of C and N isotopic compositions in IDPs, we carried out simultaneous C and N (measured as C^- and CN^-, respectively, since N^- ions are not efficiently formed) isotopic imaging measurements of an anhydrous non-cluster particle (G16) from stratospheric collector L2036 using the NanoSIMS, a new generation ion microprobe that allows isotopic imaging at a spatial scale of 100 nm. The particle, nicknamed Benavente (*16*), was pressed into a high purity Au substrate along with isotopic standards of known composition (*17*), which were measured together with the IDP on the same sample mount (*18*). The bulk C isotopic composition of Benavente is normal, with a $^{12}C/^{13}C$ of 89.3 ± 1.0 ($\delta^{13}C$ = 8 ± 11 ‰), but the IDP is enriched in ^{15}N, with an average $^{14}N/^{15}N$ ratio of 224.3 ± 1.7 ($\delta^{15}N$ = 213 ± 9 ‰) (*19*). Benavente also contains a large (0.6 x 1.8 μm^2) region that is strongly enriched in ^{15}N ($^{14}N/^{15}N$ = 119.8 ± 1.3; $\delta^{15}N$ = +1270 ± 25 ‰). This is marginally higher than the most ^{15}N-rich composition previously observed in an IDP (*10*), but what makes the anomaly particularly interesting is that the same area is depleted in ^{13}C ($^{12}C/^{13}C$ = 97.0 ± 1.2; $\delta^{13}C$ = -72 ± 12 ‰). This is illustrated in Fig. 1, which compares the C and N isotopic compositions of the anomalous region with the compositions of similar-sized areas from the rest of the image (*20*). Although the magnitude of the ^{13}C depletion is not large, its significance is emphasized by the large size of the region and its clear association with the enrichment in ^{15}N (Fig. 2). Examination of the individual layers of the image shows that both the C and N anomalies are consistently present in each of the 25 successively measured layers.

In addition to isotopic information, our NanoSIMS analysis provides some clues to the nature of the carrier phase(s) of the C and N anomaly in Benavente. The anomalous region has a significantly higher C^- yield than the rest of the IDP and a CN^-/C^- ratio of ~0.9. It is thus likely that the C and N anomalies in this region are carried by some type of organic matter. Assuming that this material is indeed carbonaceous and using the calibration curve established by (*21*), the CN^-/C^- ratio of ~0.9 suggests a N concentration of ~3.0 ± 1.5 wt.% for this area. This is at the upper end of the range of N concentrations of insoluble organic matter in carbonaceous chondrites (*15*) and falls within the field observed for CHON grains from comet Halley (*22*). Recent measurements of the $^{14}N/^{15}N$ ratios of the CN radical in the coma of two different comets give a value of 140 ± 30 (*15*), within errors the same as the $^{14}N/^{15}N$ ratio of our anomalous region.

Petrographic and Mineralogical Constraints

Using a Focused Ion Beam (FIB) technique (*23*), but we extracted a FIB section (~5 x 1 x 0.1 μm) from an area about 5 μm from the anomalous region. The area from which this section was extracted has lower C^- and CN^- signals than the anomalous region, and C and N isotopic compositions that are similar to the bulk IDP values noted above. Using a transmission electron microscope (TEM), energy-filtered imaging was employed to investigate the mineralogy of the extracted section (*24*). The energy-filtered images indicate that the region is rich in silicates (mostly GEMS, glass with embedded metal and sulfides (*25*), and minor forsterite (Mg_2SiO_4) crystals), iron-rich sulfides (pyrrhotite, $Fe_{1-x}S$), and amorphous carbonaceous material that is both clumped into distinct regions and coats some grains, such as the GEMS.

Subsequent to the TEM investigation, we used the NanoSIMS to map the distributions of C and N isotopes in the FIB slice and were able to reconfirm the ^{15}N enrichment of ~200 ‰ observed in the bulk IDP. Moreover, we found a 250 nm-sized region with a strong ^{15}N enrichment of 1110 ± 98 ‰. This enrichment was not seen in the original NanoSIMS imaging measurement because it is located below the original surface of the IDP. Correlation of this anomaly with the TEM images (Fig. 3) shows that it consists of a large area of concentrated amorphous carbonaceous material immediately

surrounded by GEMS and other silicates (a < 20 nm diameter silicate crystal observed within the carbonaceous material using lattice-fringe imaging may be forsterite). Nitrogen abundances in the FIB slice are low (1-2 wt.%), but the N is clearly associated with the carbonaceous material in this area and, thus, has an organic origin. Moreover, no other elements are associated with the N that might indicate the presence of a different carrier phase. Infrared spectra obtained from the FIB section using a synchrotron light source (*26, 27*) show a prominent C-H stretch feature at ~3.4 μm, indicative of hydrocarbons (Fig. 4). The positions of the bands within the feature are consistent with those of aliphatic hydrocarbons, but a minor aromatic hydrocarbon component cannot be ruled out. Although the ^{15}N-rich region in the FIB slice does not seem to be correspondingly ^{13}C-depleted (possibly because of the small size of the area, leading to dilution effects from surrounding isotopically normal C), the similarity of the magnitude of the N anomaly to that of the C- and N-anomalous region (as well as the proximity of the FIB slice to the original anomalous area) suggests that the same type of amorphous carbon may be the carrier of the correlated C and N anomaly.

Interstellar Organic Material

Because N (and D) isotopic anomalies in IDPs seem to be carried predominantly by organic compounds, correlated C isotopic anomalies might be expected but, prior to this study, have not been observed. Without such effects it is not possible to distinguish whether the carbonaceous material in IDPs serves as a 'recent' (*e.g.*, solar system) host substrate for presolar D and ^{15}N-enriched species, or whether the D and ^{15}N enrichments are indigenous to the (presolar) carbonaceous matter itself. Previous studies have suggested that some IDPs may contain molecular heterostructures (*13, 28, 29*), but in the absence of correlated C and N isotopic data, the origins of such molecules have remained uncertain. The correlated C and N effects that we see here show that IDPs in fact do contain complex heterostructured organic molecules of presolar interstellar origin. During its prebiotic period, the earth could have accreted as much as a centimeter of abiotic (and possibly prebiotic) carbonaceous matter every million years, much of it settling to the earth's surface within 5-50 μm diameter IDPs (*30, 31*). This constant flux

of organic matter continues to be delivered to the earth today, including interstellar molecules such as those found in Benavente.

Gas phase reactions are expected to produce C isotopic fractionations, but different processes produce fractionation effects in opposite directions (1, *32-34*). Thus, it has been suggested that the lack of C isotopic anomalies in IDPs may be due to the existence of multiple reaction pathways that cancel out any anomalies produced (*1, 34*). Others have suggested that isotopic fractionation in C may be inhibited through condensation of CO onto grain surfaces and its participation in grain chemistry (*2, 4*). Our observation of a ^{13}C depletion associated with a ^{15}N enrichment in Benavente shows that C isotopic fractionation does indeed occur and requires processes that can produce both effects in the same material. Gas phase ion-molecule reactions can enhance the $^{12}C/^{13}C$ ratios of organic species (*32, 33*) to the level observed in Benavente, but whether these reactions will also result in depleted $^{14}N/^{15}N$ ratios has not been studied. Low temperature interstellar chemistry as the source of the ^{15}N enrichments seen in IDPs has only recently been investigated theoretically. A study of various ion-molecule exchange reactions involving the most abundant N-bearing species in interstellar clouds (*8*) indicated a maximum enhancement in ^{15}N of 250 ‰. Another recent model, investigating NH_3 formation in dense molecular clouds, suggests a maximum enrichment of 800 ‰ (*9*). These models are consistent with the modest enrichment in ^{15}N seen in the bulk IDP, but fall short of the values needed to account for the +1270 ‰ enrichment in ^{15}N seen in the anomalous region. Moreover, it is not clear whether ^{15}N-rich ammonia can pass on its anomalous N to the organic hosts thought to be responsible for N isotopic anomalies in IDPs (and primitive meteorites). If future investigations of interstellar chemistry fail to account for the N (and C) isotopic fractionations observed in IDPs, circumstellar origins may need to be considered for the source of these anomalies.

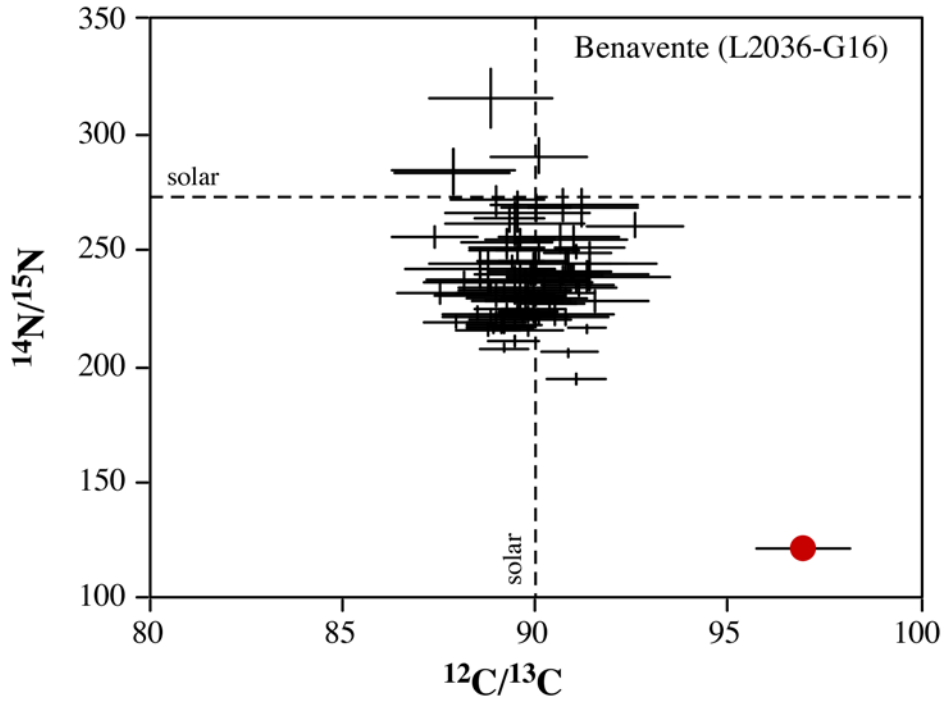

Figure 1. Isotopic composition of the anomalous region compared with similar-sized areas of Benavente. Errors are 1σ and for $^{14}N/^{15}N$ of the anomaly are smaller than the symbol. Note the spread of N isotopic compositions toward sub-solar ratios in the 'bulk' of the particle, indicating an overall enrichment in ^{15}N.

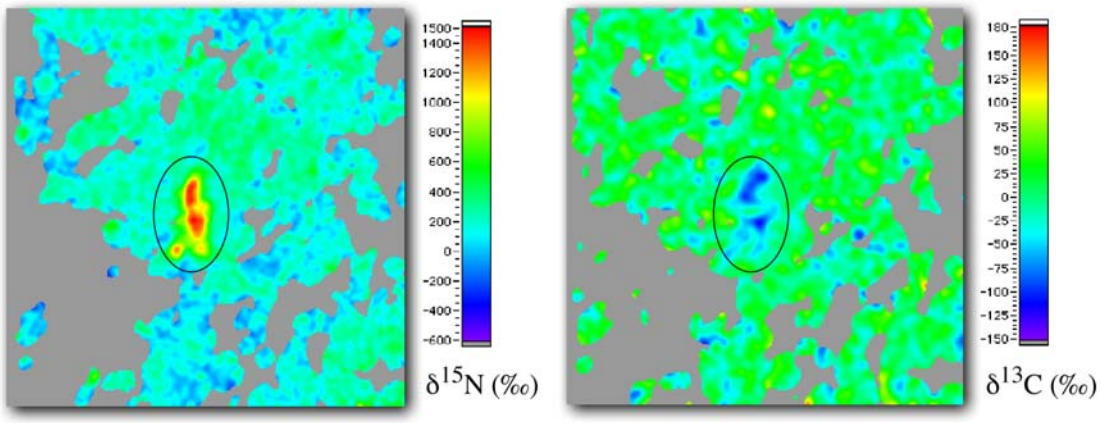

Figure 2. $\delta^{15}N$ (left) and $\delta^{13}C$ (right) images of Benavente showing the ^{15}N-enriched and ^{13}C-depleted anomalous region. Field of view is 10 µm.

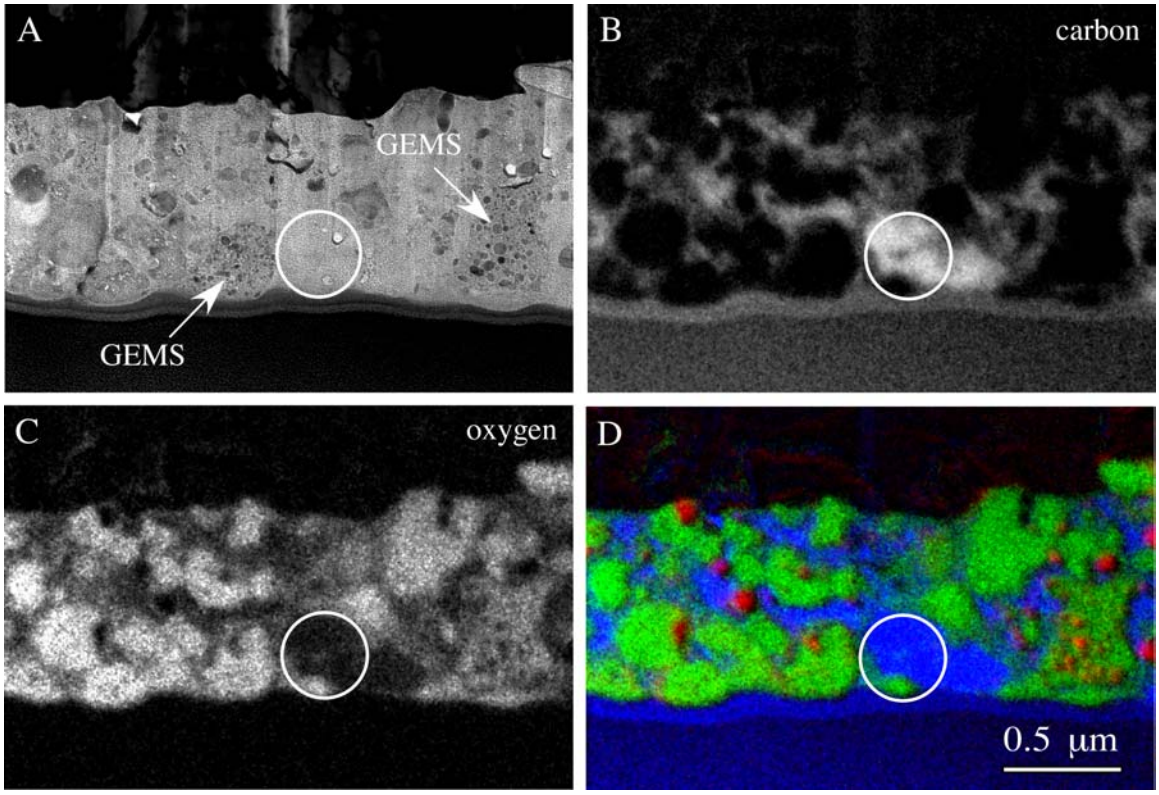

Figure 3. Images of FIB section (~ 100 nm thick) extracted from Benavente showing, in the circle, the region associated with a ^{15}N enrichment of 1110 ± 98 ‰; a) 300 keV bright-field TEM image, b) energy-filtered carbon jump ratio image, c) energy-filtered oxygen jump ratio image, and d) composite energy-filtered image showing silicates (green), carbonaceous material (blue) and iron or iron sulfides (red).

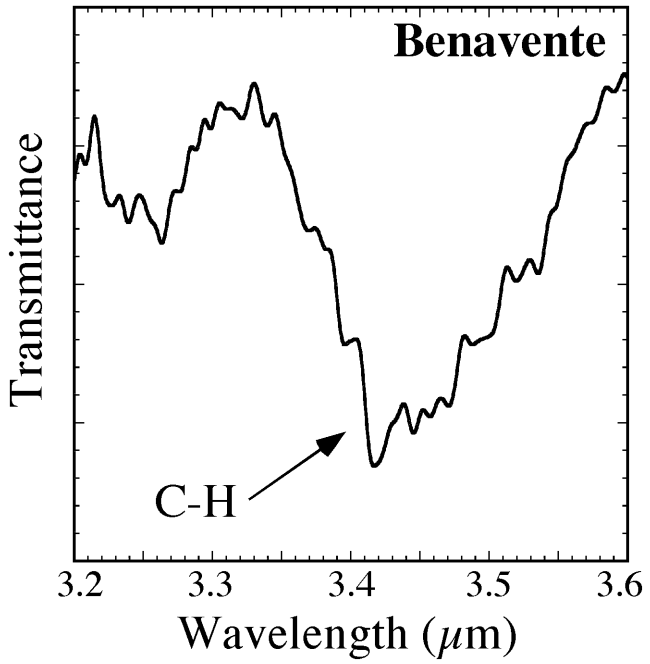

Figure 4. Synchrotron infrared (IR) spectrum obtained from the Benavente FIB section using a ~3 μm diameter incident IR beam, showing the C-H stretch feature at 3.4 μm, indicative of hydrocarbons.

References and Notes

1. A. G. G. M. Tielens, in *Astrophysical Implications of the Laboratory Study of Presolar Materials*, T. J. Bernatowicz, E. Zinner, Eds. (AIP Conf. Proc. 402, American Inst. Of Phys., Woodbury, NY, 1998), pp. 523-544.

2. S. Messenger, R. M. Walker, in *Astrophysical Implications of the Laboratory Study of Presolar Materials*, T. J. Bernatowicz, E. Zinner, Eds. (AIP Conf. Proc. 402, American Inst. Of Phys., Woodbury, NY, 1998), pp. 545-564.

3. J. P. Bradley, in *Meteorites, Planets and Comets*, A. M. Davis, Ed. (Vol. 1, Treatise on Geochemistry, H. D. Holland, K. K. Turekian, Exec. Eds., Elsevier Science, 2003), in press.

4. S. Messenger, F. J. Stadermann, C. Floss, L. R. Nittler, S. Mukhopadhyay, *Space Sci. Rev.* **106**, 155 (2003).

5. T. J. Millar, A. Bennett, E. Herbst, *Astrophys. J.* **340**, 906 (1989).

6. S. Messenger, *Nature* **404**, 968 (2000).

7. C. M. O'D. Alexander *et al*., *Meteorit. Planet. Sci.* **33**, 603 (1998).

8. R. Terzieva, E. Herbst, *Mon. Not. R. Astron. Soc.* **317**, 563 (2000).

9. S. B. Charnley, S. D. Rodgers, *Astrophys. J.* **569**, L133 (2002).

10. C. Floss, F. J. Stadermann, *Lunar Planet. Sci.* **33**, #1350 (2002).

11. C. Floss, F. J. Stadermann, *Lunar Planet. Sci.* **34**, #1238 (2003).

12. S. Mukhopadhyay, L. R. Nittler, *Lunar Planet. Sci.* **34**, #1941 (2003).

13. L. P. Keller, S. Messenger, M. Miller, K. L. Thomas, *Lunar Planet. Sci.* **28**, 707 (1997).

14. J. Aléon, F. Robert, M. Chaussidon, B. Marty, C. Engrand, *Lunar Planet. Sci.* **33**, #1397 (2002).

15. J. Aléon *et al.*, *Lunar Planet. Sci.* **34**, #1308 (2003).

16. Jacinto Benavente won the Nobel Prize for Literature in 1922 for his contributions to Spanish drama.

17. 1-hydroxybenzotriazole hydrate was used as a standard for both C and N measurements.

18. A ~2 pA 16 keV Cs^+ beam was rastered over a 10 x 10 μm^2 area while secondary ions ($^{12}C^-$, $^{13}C^-$, $^{12}C^{14}N^-$, $^{12}C^{15}N^-$ and $^{28}Si^-$) were collected simultaneously in five electron multipliers at a mass resolution ($m/\Delta m$ ~6500) sufficient to separate the neighboring $^{10}B^{16}O^-$ and $^{11}B^{16}O^-$ peaks from $^{12}C^{14}N^-$ and $^{12}C^{15}N^-$, respectively. A larger 40 x 40 μm^2 scan over the entire particle surface initially identified the isotopically anomalous region of interest. Isotopic imaging measurements typically consist of 10 to 40 scans that are subsequently added together to constitute a single image, thus avoiding potential data loss problems caused by the artificial limit of 2^{16} counts/pixel set by the counting system of the NanoSIMS and allowing observed isotopic anomalies to be verified through the different layers. The data were processed using custom software written in Labview. Images were corrected for sample drift from layer to layer and were checked for statistical outliers. Isotopic ratios and errors were calculated following standard conventions.

19. Delta values represent the deviation of the measured isotopic ratio from the value of the terrestrial standard in parts per thousand (‰). Terrestrial ratios are $^{12}C/^{13}C = 90$ and $^{14}N/^{15}N = 272$.

20. The particle was divided into 94 randomly generated sub-regions similar in size and shape to the anomalous region, with analytical errors (1σ) of 4% or less for both $^{14}N/^{15}N$ and $^{12}C/^{13}C$.

21. J. Aléon, F. Robert, M. Chaussidon, B. Marty, *Geochim. Cosmochim. Acta* **67**, 3773 (2003).

22. M. N. Fomenkova, S. Chang, L. M. Mukhin, *Geochim. Cosmochim. Acta* **58**, 4503 (1994).

23. P. J. Heaney, E. P. Vicenzi, L. A. Giannuzzi, K. J. T. Livi, *Am. Mineral.* **86**, 1094 (2001).

24. The section was examined using 200 and 300 keV field emission transmission electron microscopes (Phillips CM 200 and CM 300 series). Bright-field and dark-field imaging, electron diffraction, lattice-fringe imaging, energy-dispersive X-ray spectroscopy and electron energy-loss spectroscopy were employed to investigate compositions, mineralogy and petrography. The section was also compositionally mapped for C, N, O, Mg, Al, Si, S, Fe and Ni using x-ray mapping, and energy-filtered

imaging for C, N, O and Fe. Both methods provide compositional images with ~2 nm spatial resolution. Energy-filtered transmission electron microscopy (EFTEM) images were obtained with a Gatan Imaging Filter (GIF) setting energy windows at pre-edges and post-edges of the C–K, O–K and Fe–$L_{2,3}$ core ionizations, respectively. A 10 eV energy window was selected for C, a 20 eV window for O and a 25 eV window for Fe. The EFTEM images were acquired using a 3 mm GIF entrance aperture. Digital Micrograph (v. 3.3.1) was used to obtain, correlate and divide post-edge images by pre-edge images, resulting in the 'jump-ratio' images shown in Fig. 3. All images were recorded using a slow-scan charge-coupled-device (CCD) camera (1024 x 1024 pixels).

25. J. P. Bradley, *Science* **265**, 925 (1994).

26. The infrared measurements were performed with the infrared spectromicroscopy beamline 1.4.3 at the Advanced Light Source, Lawrence Berkeley National Laboratory. A detailed description of the beamline is given by [27]. Multiple sets of spectra were acquired in transmission mode with 8 cm^{-1} resolution and 1026 scans per spectrum. Each spectrum was acquired over a 600 – 1000 cm^{-1} energy range. The beam spot of the beamline is diffraction-limited and in the region of interest (~2900 cm^{-1}) measures about 3 μm. The observed features at 3.4 μm (2925 cm^{-1}) and 3.44 – 3.5 μm (2900 – 2850 cm^{-1}) shown in Fig. 4 are characteristic of C–H_2 stretching vibrations in an aliphatic hydrocarbon.

27. M. C. Martin, W. R. McKinney, *Ferroelectrics* **249**, 1 (2001).

28. S. J. Clemett, C. R. Maechling, R. N. Zare, P. D. Swan, R. M. Walker, *Science* **262**, 721 (1993).

29. G. J. Flynn, L. P. Keller, D. Joswiak, D. E. Brownlee, *Lunar Planet. Sci.* **33**, #1320 (2002).

30. D. E. Brownlee, in *Analysis of Interplanetary Dust*, M. E. Zolensky, T. L. Wilson, F. Y. M. Rietmeijer, G. J. Flynn, Eds. (AIP conf. Proc. 310, American Inst. Of Phys., Woodbury, NY, 1994), pp. 5-8.

31. D. E. Brownlee, D. J. Joswik, M. E. Kress, S. Taylor, J. Bradley, *Lunar Planet. Sci.* **33**, #1786 (2002).

32. W. D. Langer, T. E. Graedel, M. A. Frerking, P. B. Armentrout, *Astrophys. J.* **277**, 581 (1984).

33. W. D. Langer, T. E. Graedel, *Astrophys. J.* **69**, 241 (1989)

34. S. A. Sandford, M. P. Bernstein, J. P. Dworkin, *Meteorit. Planet. Sci.* **36**, 1117 (2001).

35. This work was supported by NASA grants NAG5-13467 to C. Floss, and NAG5-10623 and NAG5-10696 to J. Bradley. Electron microscopy was performed under the auspices of the U.S. Department of Energy by University of California, Lawrence Livermore National Laboratory under contract No. W-7405-Eng-48, and at the National Center for Electron Microscopy at Lawrence Berkeley Laboratory (supported by DoE contract No. DEAC03-76SF000098). Infrared spectroscopy was performed at the Advanced Light Source at Lawrence Berkeley National Laboratory (supported by DoE contract No. DE-AC03-76SF00098). The authors would like to thank T. Smolar of Washington University for NanoSIMS maintenance and support, M. Martin and the ALS personnel for providing the ALS beamline, and K. Moore at LLNL for assistance with energy-filtered imaging.